OPEN ACCESS

Opin vísindi

This is not the published version of the article / Þetta er ekki útgefna útgáfa greinarinnar

Author(s)/Höf.: Juhl, M., Mueller, J. P. B., & Leosson, K

Title/Titill: Metasurface Polarimeter on Optical Fiber Facet by Nano-Transfer to UV-Curable Hybrid Polymer

Year/Útgáfuár: 2019

Version/Útgáfa: Post-print (lokagerð höfundar)

Please cite the original version:

Vinsamlega vísið til útgefnu greinarinnar:

Juhl, M., Mueller, J. P. B., & Leosson, K (2019). Metasurface Polarimeter on Optical Fiber Facet by Nano-Transfer to UV-Curable Hybrid Polymer. *IEEE Journal of Selected Topics in Quantum Electronics, 25*(3), 1-7. doi: 10.1109/JSTQE.2019.2893757

Rights/Réttur: © 2019 IEEE

This article has been accepted for publication in a future issue of this journal, but has not been fully edited. Content may change prior to final publication. Citation information: DOI 10.1109/JSTQE.2019.2893757, IEEE Journal of Selected Topics in Quantum Electronics

Metasurface Polarimeter on Optical Fiber Facet by Nano-Transfer to UV-Curable Hybrid Polymer

Michael Juhl, Jan Philipp Balthasar Mueller and Kristjan Leosson

***Abstract*—A simple, cost-effective, and high-throughput method of patterning an optical fiber facet using template stripping to transfer a gold pattern to a UV-curable hybrid polymer is presented. The template stripping transfer method is demonstrated with two different approaches: A fiber exposure approach where the position of the transferred nanostructure relative to the fiber can be aligned by optical curing of polymer through the fiber, and a flood exposure approach that allows the transfer of a larger area of nanostructure. An in-line metasurface polarimeter patterned on a 1550 nm single-mode fiber facet using this technique is reported, demonstrating the capacity of the miniaturization of the metasurface polarimeter. The demonstrated fiber-based metasurface polarimeters are ultra-compact, cost-effective, robust, simple, and deliver high-performance polarization measurements. They are fully viable alternatives to existing solutions with applications mainly in polarization state generation and fiber optics communication.**

***Index Terms*—Nanostructured fibers, Polarimetry, Optical metasurfaces, Transfer nanolithography.**

I. Introduction

METASURFACES are quasi-two-dimensional optical nanostructures that enable spatially dependent tailoring of the amplitude, phase or polarization of light. There has been a growing interest in this new class of optically engineered nanostructures over the past few years as a result of reports of unconventional light-matter interaction and the promise of miniaturization of optical components [1]–[4]. Integration of nanostructures onto optical fiber facets has the potential of opening new applications for highly miniaturized optical devices, such as surface-enhanced Raman scattering sensors, surface-plasmon-resonance sensors, beam steering structures, fiber optical tweezers, polarization state generators, and devices for polarization monitoring in telecommunications networks [5]–[7].

Fabricating nanoscale structures on a fiber tip is a challenging task. The large aspect ratio and microscopic cross-section of the fiber are not compatible with conventional wafer-based processing platforms, originating from the semiconductor industry. Instead, many different approaches have been demonstrated, employing technologies such as focused ion beam milling, nanoimprinting, two-photon polymerization, and transfer lithography [8]–[10].

Transfer lithography techniques offer convenient methods of high-resolution optical fiber tip patterning suitable for parallel processing. Many of the reported methods, however, require complicated processing like mold preparation, manual transfer by mechanical contact, or multiple film delamination [11]–[13]. In this work we demonstrate a simple nano-transfer technique that we use to define patterns of metallic nanoantennas on fiber facets. The method involves only a few simple processing steps, easy alignment and potential for low-cost production.

Metasurfaces enable the fabrication of planar optical components, thereby in many cases reducing the cost, size, and complexity of existing devices. A few examples are flat lenses [14]–[16], spectrometers [17], and polarimeters [18]–[20]. A particular instance of devices for polarization measurement is the in-line polarimeter, which performs non-terminating polarization measurements of optical signals. Whereas current in-line polarimeters are constructed with multiple optical components in series [21], a metasurface polarimeter requires only one ultrathin surface of nanoantennas [18], while matching state-of-the-art fiber-based in-line polarimeters in terms of speed and precision. In-line polarimeters play a critical role in monitoring and controlling the polarization in optical communication networks. Integrating the metasurface polarimeter on an optical fiber would therefore not only represent an important step towards the ultimate miniaturization of the polarimeter but also be very useful in applications like optical networks.

II. Fabrication

The principle of the template stripping transfer processes is illustrated in Fig. 1. The metasurface pattern was initially written into a layer of polymethyl methacrylate (PMMA) on a

Manuscript received August 15, 2018. This work was supported in part by Icelandic Research Fund (152098051) and Air Force Office for Scientific Research (AFOSR), MURI Grant (FA9550-14-1-0389, FA9550-16-1-0136).

Michael Juhl is with Innovation Center Iceland and University of Iceland, Reykjavík, Iceland (e-mail: michael.juhl@nmi.is).

J. P. Balthasar Mueller is with Harvard School of Engineering and Applied Sciences, Cambridge, MA 02138 USA (e-mail: jpbm@seas.harvard.edu).

Kristjan Leosson is with Innovation Center Iceland and University of Iceland, Reykjavík, Iceland (phone +354-522-9000; e-mail: kristjan.leosson@nmi.is).

1077-260X (c) 2018 IEEE. Personal use is permitted, but republication/redistribution requires IEEE permission. See http://www.ieee.org/publications_standards/publications/rights/index.html for more information.

This article has been accepted for publication in a future issue of this journal, but has not been fully edited. Content may change prior to final publication. Citation information: DOI 10.1109/JSTQE.2019.2893757, IEEE Journal of Selected Topics in Quantum Electronics

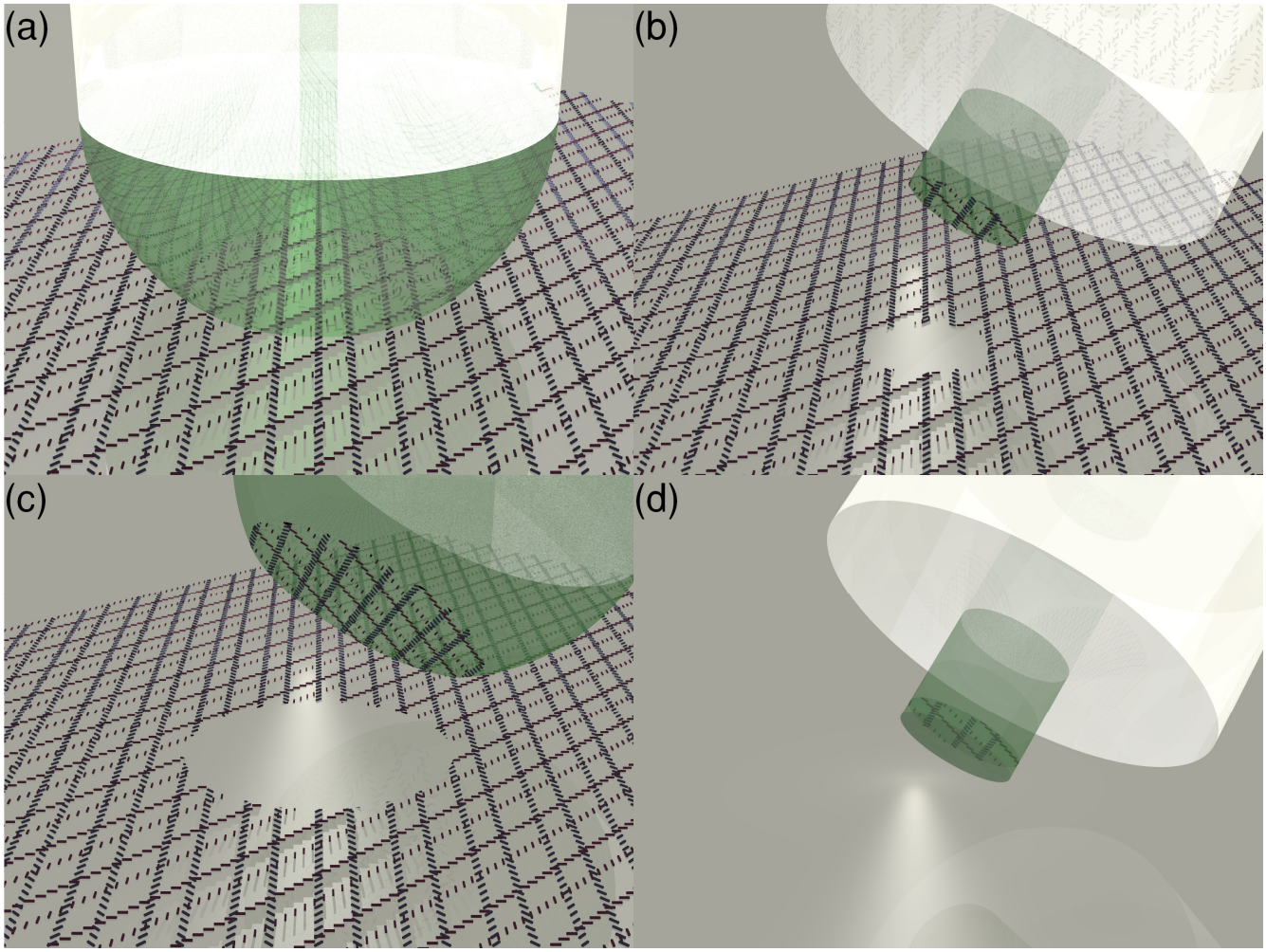

Fig. 1. (a) An optical fiber (white cylinder) with a drop of polymer (green hemisphere) on the tip in proximity to a metasurface consisting of arrays of gold nanoantennas. The metasurface is made of two superimposed gratings of antenna columns arranged in a pattern where the antennas in each column are rotated 90° relative to antennas in the neighboring column. (b) The polymer is UV-cured through the fiber core resulting in only the antennas under the center of the fiber being released from the wafer. (c) The polymer is UV-cured using flood exposure resulting in a larger metasurface area being released from the surface. (d) A second layer of polymer is cured on top of the existing polymer. The polymer is cured on an unstructured surface to ensure a flat end face.

silicon wafer using electron beam lithography. Gold was subsequently deposited on the resist and patterned in a lift-off process. A 1550-nm single-mode fiber was mechanically cleaved, dipped in a UV-curable organic/inorganic hybrid polymer (OrmoComp®, micro resist technology GmbH), leaving a droplet of polymer on the fiber tip, and brought into near proximity to the patterned silicon wafer (Fig. 1a). The polymer was then cured with 365-nm ultraviolet light using one of two approaches. With the fiber exposure approach the UV-light was transmitted through the fiber itself, thus forming a cylindrical polymer rod between the fiber and the wafer as a result of confinement within the fiber and a self-guiding phenomenon within the optically-cured polymer. After UV exposure, the fiber was retracted, delaminating the gold from the wafer and transferring it to the surface of the cured polymer rod, as a result of low adhesion between gold and silicon. This simple delamination process is known as template stripping [22], [23]. Template stripping uses the fact that some metals, gold included, have low adhesion when deposited directly on silicon. The adhesion is high enough that structures do not delaminate during the liftoff process, but low enough that stripping from the wafer is straightforward. UV-curing through the fiber ensures that the nanostructure is automatically transferred only to the area corresponding to the fiber-core (Fig. 1b). Uncured polymer was removed with a developer (OrmoDev®, micro resist technology GmbH). Fig. 1c illustrates an alternative flood-exposure approach where the polymer was cured from outside the fiber, thus curing the entire droplet of polymer on the fiber tip. The metasurfaces transferred to the polymer rod can subsequently be fully embedded in polymer by repeating the process using a clean silicon wafer without nanoantennas. This is illustrated in Fig. 1d with the fiber exposure approach.

Electron micrograph images of the patterned fibers are shown in Fig. 2. The diameter of the polymer rod in Fig. 2a is $10-10.5\,\mu m$ corresponding well to the core size of an SMF-

1077-260X (c) 2018 IEEE. Personal use is permitted, but republication/redistribution requires IEEE permission. See http://www.ieee.org/publications_standards/publications/rights/index.html for more information.

This article has been accepted for publication in a future issue of this journal, but has not been fully edited. Content may change prior to final publication. Citation information: DOI 10.1109/JSTQE.2019.2893757, IEEE Journal of Selected Topics in Quantum Electronics

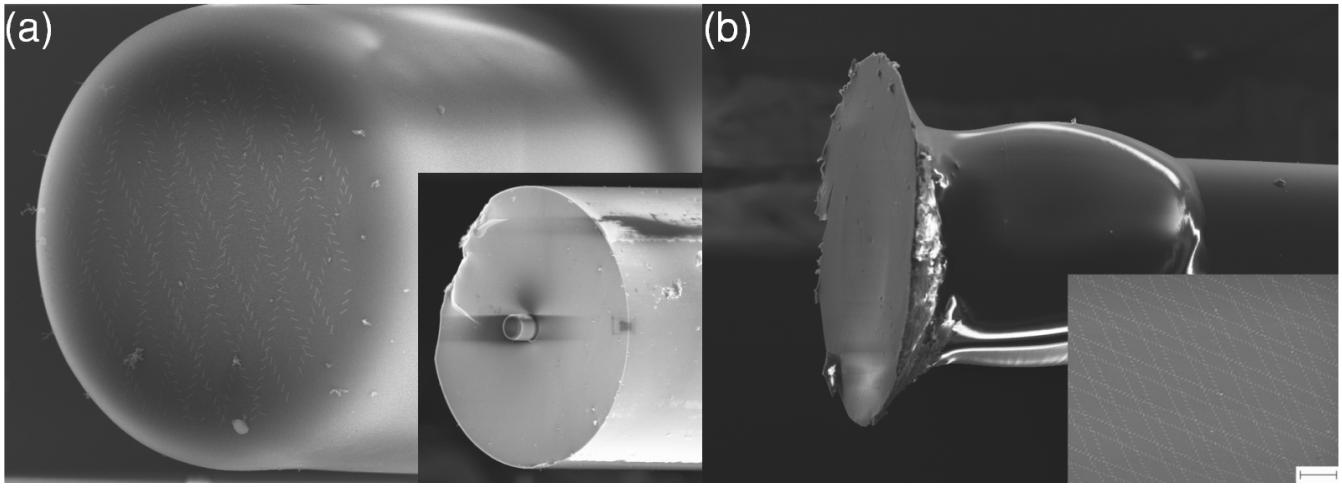

Fig. 2. Micrograph images of patterned fibers. (a) Image of a polarimeter fabricated with the fiber exposure approach, showing the 10 µm-diameter polymer rod with gold nanoantennas on the top. The inset shows a zoom-out of the entire fiber tip that has diameter of 125 µm. (b) Image of a patterned fiber facet using the flood exposure approach, where a much larger area of nanoantennas arrays is transferred. The inset shows a zoom-in of the transferred nanoantenna arrays (the scale bar represents a length of 2 µm).

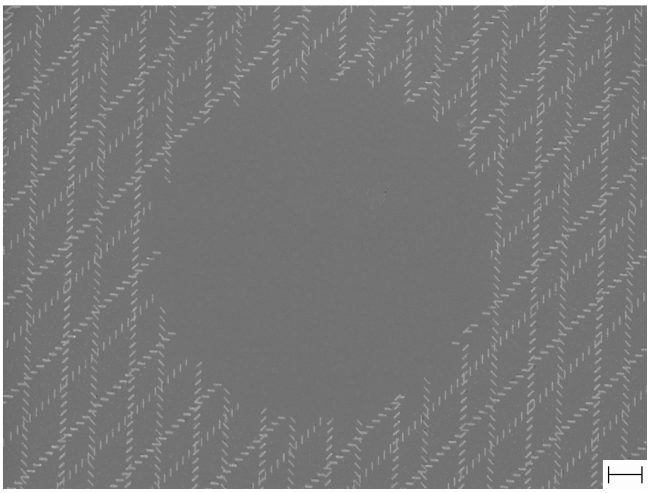

Fig. 3. Electron micrograph of metasurface on a silicon wafer after stripping. In the middle of the image is a circle with a diameter of about 10 µm, where the gold nanoantennas have been transferred to the fiber tip. The scale bar represents a length of 1 µm.

28 optical fiber. Fig. 3 shows a micrograph of the silicon wafer after transfer lithography with the fiber exposure approach. It is observed that all antennas in a circular area, corresponding to the mode size of an SMF-28 optical fiber, are successfully detached from the sample.

III. Polarimeter on a Fiber Facet

We have previously presented a new in-line, polarization preserving polarimeter design [18] based on an optical metasurface formed by arrays of nanoantennas [24]. Identical gold nanorods (250 nm x 50 nm x 20 nm) are arranged with subwavelength-spacing in parallel arrays (see Figs. 2 and 3). The metasurface consists of two antenna arrays with columns of antennas, individually oriented ±45° with respect to the orientation of the columns of each array. The distance between the two columns of perpendicularly oriented antennas is $\lambda(1+1/4)$ and the column-pairs are spaced 2λ, where λ is the design wavelength in the polymer material, corresponding also roughly to the resonance wavelength of the individual antennas. When near-infrared light (C-band wavelengths) is normally incident on the metasurface, a fraction of the intensity is scattered in polarization-dependent in-plane and out-of-plane meta-grating orders; each order serving as a polarization analyzer [25]. The in-plane grating orders stay in the plane of the metasurface, whereas light in the out-of-plane orders is scattered at an angle close to 45° from the metasurface plane after refraction at the polymer/air interface. Only out-of-plane orders are used for intensity measurements, since in-plane orders suffer from lensing and scattering from imperfections at the edge of the structure. The rescattering of the in-plane orders at the fiber-cladding/air interface is observed in images in Fig. 4 using an infrared camera and a reflective microscope objective from Ealing. Aside from mapping the fiber facet to the image plane, the reflective objective serves to block most of the light from the fiber to avoid overexposing the image. The images of the rescattering demonstrate the polarization-dependent light scattered by the metasurface.

The transfer lithography processes allow for two different polarimeter designs, a fiber exposure design that is self-aligned to the fiber core and a flood exposure design, as illustrated in Figs. 1b and 1c. Obviously, the fiber exposure design is the most compact solution and transfers a far smaller area of the patterned gold than the flood exposure design. However, the signal intensity of the self-aligned polarimeter is much smaller than the intensity from the flood exposure polarimeter due to increased scattering from the polymer cylinder itself and the smaller overall number of antennas. This results in larger error on the measured Stokes vector.

1077-260X (c) 2018 IEEE. Personal use is permitted, but republication/redistribution requires IEEE permission. See http://www.ieee.org/publications_standards/publications/rights/index.html for more information.

This article has been accepted for publication in a future issue of this journal, but has not been fully edited. Content may change prior to final publication. Citation information: DOI 10.1109/JSTQE.2019.2893757, IEEE Journal of Selected Topics in Quantum Electronics

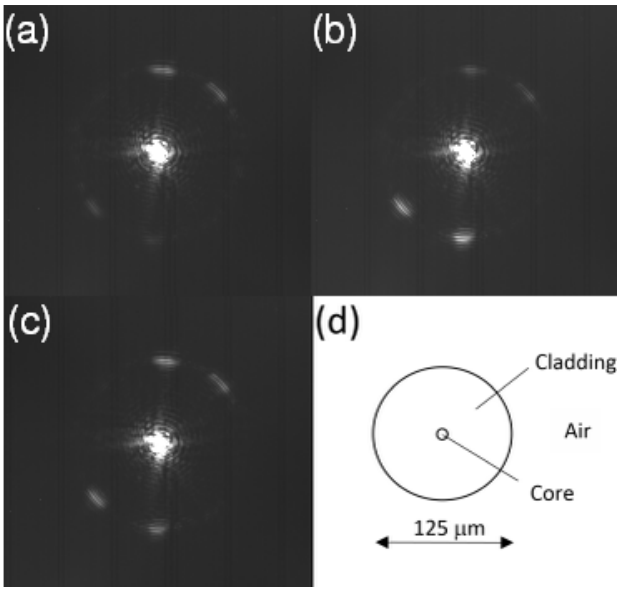

Fig. 4. Fiber-cladding images of an optical fiber facet patterned with a flood exposure metasurface polarimeter design. In-plane orders are seen rescattered out of plane at the fiber-cladding/air interface. The bright spot in the middle is the light emitted from the fiber that escapes being blocked by the reflective objective. The relative intensity of scattered orders varies with the polarization of the incoming light. (a) Right-hand circular polarization. (b) Left-hand circular polarization. (c) Horizontal linear polarization. (d) Schematic of fiber facet showing the dimensions of the cladding.

The patterned optical fiber was connected to a fiber laser at a wavelength of 1550 nm, followed by a deterministic polarization controller (DPC). The intensity of four out-of-plane orders was measured to obtain information about the polarization of the incoming light. The full information about the polarization is contained in the 4-element Stokes vector [26]. Output intensity is related to the polarization by a 4-by-4 analyzer matrix, which is found by calibration to known polarizations [27]. With at least four intensity measurements the Stokes vector of the incoming light can therefore be reconstructed using a linear transformation. Four InGaAs photodiodes were fitted in a 3D-printed holder and aligned to the scattered light from the grating orders with the help of an xyz stage. The out-of-plane grating orders can be observed in Fig. 5. The images were recorded with arbitrary brightness by placing the structured fiber directly in front of the infrared camera. The signal from the diodes was amplified and sampled using a microcontroller that collected 300-sample sets at a rate of 1 kHz [25]. The transmitted light was coupled back into a second fiber, which was attached to another xyz stage and positioned approximately 100 µm from the metasurface, obtaining a coupling efficiency of about 50 % (-3 dB) where about 3 % can be related to reflection losses. The unstructured fiber was connected to a commercial in-line polarimeter (IPL). Since transmission through the optical fibers affects the polarization of the light, the polarization at the metasurface polarimeter and the in-line polarimeter were calibrated to the polarization set by the DPC using a commercial free-space polarimeter (POL) and two manual polarization controllers

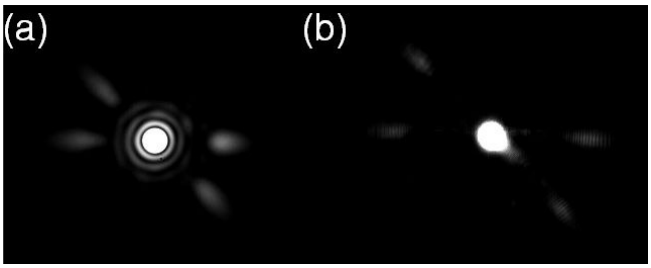

Fig. 5. Images of the out-of-plane orders for (a) fiber exposure design and (b) flood exposure design.

(MPC), which were placed on the fibers before and after the metasurface polarimeter. First the MPC on the metasurface fiber was employed to calibrate the polarization at the position of the metasurface to the DPC by removing the fiber attached to the IPL and measuring the output polarization with the POL. Then the unstructured fiber was aligned to the metasurface fiber and the polarization of the IPL was calibrated to the DPC using the MPC on the unstructured fiber. Schematics of the measurement setup are shown in Fig. 6 together with measurements from the metasurface polarimeter with the fiber exposure design. The results in Fig. 6c consist of polarization states measured by the metasurface fiber polarimeter, reference polarizations measured by the deterministic polarization controller, and polarization measurements using the in-line polarimeter; all represented on the same Poincaré sphere, viewed from opposing angles. The discrepancy between the DPC and the IPL polarization measurements is caused by inaccuracy in correction of polarization changes in the fiber (a 3-dimensional rotation on the Poincaré sphere) and polarization-dependent losses between the DPC and the IPL that causes a slight asymmetry of the polarization measurements on the Poincaré sphere (they are stretched towards the polarization state with the highest transmission). The root-mean-square error (RMSE) between measured and reference polarizations on all state-of-polarization parameters for the fiber exposure device was around 0.006. This corresponds to an error of 0.19° on the azimuth angle of the polarization ellipse and 0.28° on the ellipticity angle. Conversely, the RMSE of the Stokes parameters for the device made using the flood exposure method was around 0.004 or 0.23° on the azimuth angle and 0.15° on the ellipticity. The lower error with the flood exposure approach is expected, due to an increased signal to the detectors. The difference in error between the flood exposure design and the fiber exposure design is, however, smaller than expected because the polarization-dependent fraction of the total scattered intensity with the fiber exposure method is larger when compared to the flood exposure method. The RMSE obtained with the fiber-based metasurface polarimeters corresponds to the same level of precision that we earlier obtained with 4-output metasurface polarimeters on fused silica wafers (see appendix), implying that transferring the metasurface to the tip of a fiber does not deteriorate the performance of the polarimeter. The accuracy of the metasurface polarimeter is comparable to the state-of-

1077-260X (c) 2018 IEEE. Personal use is permitted, but republication/redistribution requires IEEE permission. See http://www.ieee.org/publications_standards/publications/rights/index.html for more information.

This article has been accepted for publication in a future issue of this journal, but has not been fully edited. Content may change prior to final publication. Citation information: DOI 10.1109/JSTQE.2019.2893757, IEEE Journal of Selected Topics in Quantum Electronics

the-art in-line polarimeter from Thorlabs (IPM5300) that has an accuracy of ±0.25° on the state-of-polarization parameters at an incoming power of 1 – 2 mW and an averaging time larger than 1 ms. 11 % of the total incoming power is lost in the polarization measurement of the IPM5300 (excluding loss at optical connectors). 28 – 29 % of the total incoming power is lost in the metasurface polarimeters. The scattered and absorbed power in the metasurface is approximately equal [28] and the scattered power is distributed to a total of 16 scattering orders [25]. The power arriving at each detector is 0.4 – 0.5 % of the total incoming power in case of the flood exposure design and 0.1 – 0.2 % in case of the fiber exposure design. These results show that the template stripping transfer lithography method is an effective method for fabricating high quality optical componts and they suggest that a fiber-based metasurface in-line polarimeter is a viable alternative to in-line polarimeters based on, e.g., pairs of tilted fiber Bragg gratings separated by birefringent fiber sections. Due to the inherent wavelength sensitivity of the metasurface design, the polarization can only be accurately determined if the input wavelength is within approximately 0.1 nm of the calibration wavelength [28]. By using deep neural networks trained on

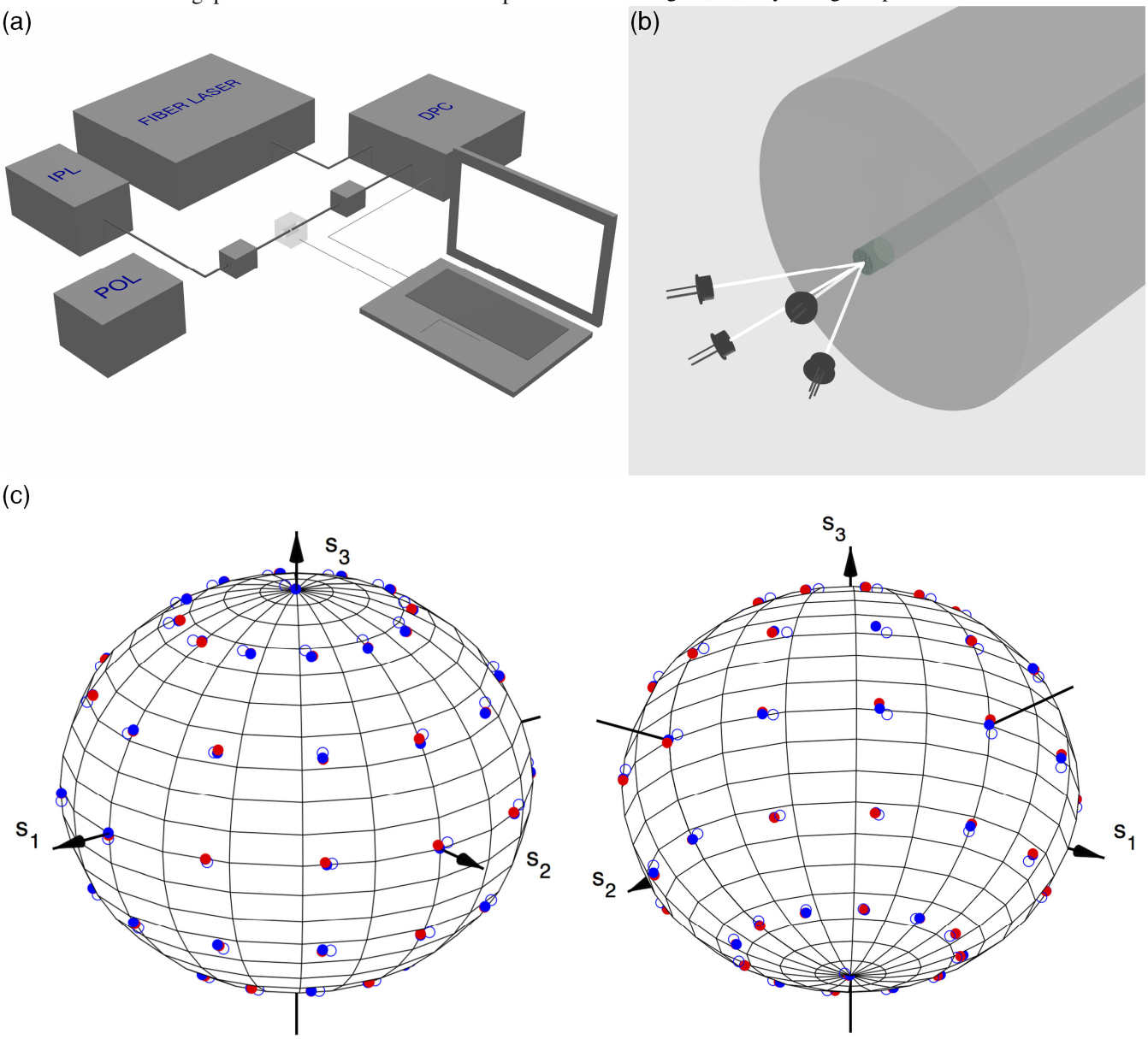

Fig. 6. (a) A schematic of the measurement setup showing a fiber laser connected to a deterministic polarization controller (DPC) with a 1550 nm single-mode fiber. The nanostructured fiber is connected to the output of the DPC and aligned to four photodiodes using a 3D-printed holder (the semitransparent box). An optical fiber with an unstructured tip is aligned to the nanostructured fiber to couple the signal into a commercial in-line polarimeter (IPL). The commercial free-space polarimeter (POL) and the manual polarization controllers (the two small boxes on the fibers) are used to calibrate the polarization. (b) The configuration of the photodetectors is illustrated. The diodes are scaled down in size relative to the fiber. (c) Measurements of the polarization state depicted on a Poincaré sphere, viewed from two opposite angles. Red dots are measurements using the metasurface polarimeter with the fiber exposure design, blue dots are reference polarization states measured by the DPC. The open blue circles are polarization states measured by the IPL.

1077-260X (c) 2018 IEEE. Personal use is permitted, but republication/redistribution requires IEEE permission. See http://www.ieee.org/publications_standards/publications/rights/index.html for more information.

This article has been accepted for publication in a future issue of this journal, but has not been fully edited. Content may change prior to final publication. Citation information: DOI 10.1109/JSTQE.2019.2893757, IEEE Journal of Selected Topics in Quantum Electronics

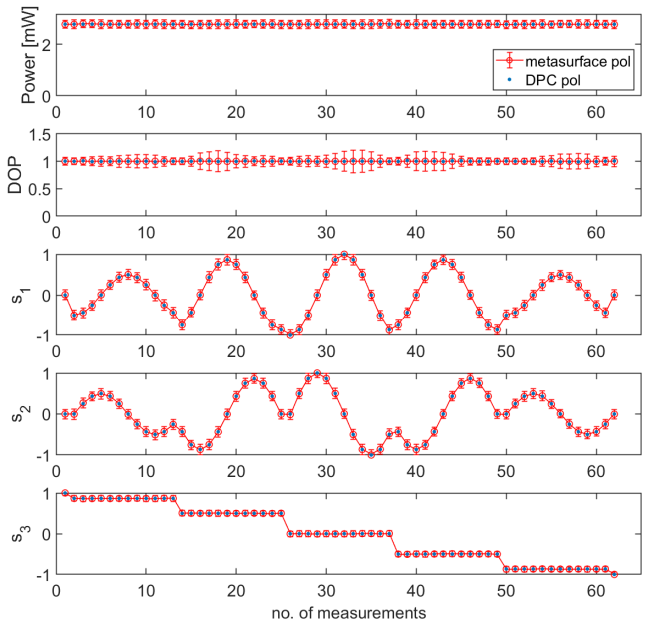

Fig. A1. Polarization measurements at a wavelength of 1550 nm using a wafer-based metasurface polarimeter. The first subplot is the power of the incident light, which is proportional to the first element of the Stokes vector, S_0. The next subplot is the degree of polarization (DOP) and the three last subplots are the parameters characterizing the state of polarization (SOP), s_1 – s_3. The red circles are the polarization measurements of the metasurface polarimeter, the blue dots are the reference polarizations set by the deterministic polarization controller (DPC). Standard deviation on the reference polarization measurements is not depicted on the plot, since the size of the error bars would be smaller than the size of the marker.

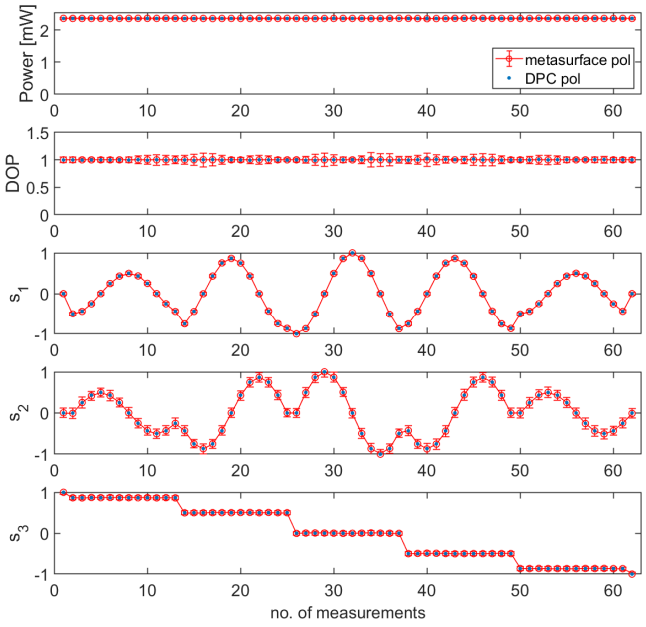

Fig. A2. Polarization measurements at 1550 nm using the fiber-based flood exposure metasurface polarimeter.

calibration data, we have shown that the metasurface polarimeter can accurately measure polarization over a wide wavelength range without a-priori knowledge of input wavelength, and the functionality of the polarimeter can simultaneously be enhanced to measure the input wavelength as well [29].

IV. Conclusion

We have presented a new transfer-lithography process based on template stripping for nanostructuring of optical fiber facets. The applicability of this novel approach has been demonstrated by transferring a 4-output metasurface polarimeter to the facet of a 1550 nm single-mode fiber. The results show that the performance of the metasurface polarimeter is not negatively affected by the transfer from a wafer to an optical fiber.

The metasurface polarimeter-on-a-fiber is an excellent candidate for telecommunication applications with exceptional stability and compactness and no subsequent pigtailing requirements. The presented transfer technique may also be useful for sensor applications, such as fiber-based surface-enhanced Raman scattering probes and surface-plasmon-resonance sensors. By including active alignment of the silicon wafer base, the future prospect of the technique also includes integration of wavefront shaping elements like flat lenses and q-plates (spin-to-orbital angular momentum converters) directly onto the fiber facet. Furthermore, the demonstration of multiple-layer hybrid polymer structures opens for fiber-based devices with several consecutive layers of metasurfaces.

Appendix

We compare the performance of the fiber-based metasurface polarimeters with the performance of a fiber-coupled wafer-based metasurface polarimeter. The antenna arrays of the wafer-based metasurface polarimeter are embedded in layers of benzocyclobutene (BCB) polymer on top of a fused silica wafer. More fabrication details can be found in [25]. Polarization measurements (red circles) of a wafer-based polarimeter are shown in Fig. A1 together with reference polarization (blue dots). The polarimeter is measured in an out-of-plane configuration. Measurements using the two different fiber-based metasurface polarimeter designs are shown in Figs. A2-A3 for comparison. The uncertainty on the polarization measurements (red error bars) is calculated from uncertainty in the intensity measurements and from error propagation through the calibration process using the general error propagation formula [30]. The uncertainty of the degree of polarization (DOP) is calculated from the uncertainty of the Stokes parameters [31].

1077-260X (c) 2018 IEEE. Personal use is permitted, but republication/redistribution requires IEEE permission. See http://www.ieee.org/publications_standards/publications/rights/index.html for more information.

This article has been accepted for publication in a future issue of this journal, but has not been fully edited. Content may change prior to final publication. Citation information: DOI 10.1109/JSTQE.2019.2893757, IEEE Journal of Selected Topics in Quantum Electronics

The root-mean-square error (RMSE) between polarization states measured by the wafer-based metasurface polarimeter and reference polarization states for the wafer-based polarimeter is 0.005. We can therefore conclude that we have obtained the same level of precision with the fiber-based polarimeter as with the wafer-based polarimeter. It should be noted, however, that the variation in the polarization response between the polarization analyzers of the three devices affects the error and causes an uncertainty in the RMSE. Also the variance of the measured intensities, caused by electronic noise, is higher for the wafer-based metasurface polarimeter.

ACKNOWLEDGMENT

The authors acknowledge the fruitful collaboration with Prof. Federico Capasso of Harvard SEAS. The results in this article is based on his pioneering work on metasurfaces. The authors thank Carlos Mendoza (Innovation Center Iceland) for help with the characterization setup and Kesara M. Jónsson (University of Iceland) for help with SEM imaging. M. Juhl thanks Noah Rubin (Harvard SEAS) and Rou Ping Li (University of Waterloo) for helpful discussions about polarimetry.

REFERENCES

[1] P. Lalanne, S. Astilean, P. Chavel, E. Cambril, and H. Launois, "Design and fabrication of blazed binary diffractive elements with sampling periods smaller than the structural cutoff," *J. Opt. Soc. Am. A*, vol. 16, pp. 1143-1156, 1999.

[2] N. Yu and F. Capasso, "Flat optics with designer metasurfaces," *Nat. Mat*, vol. 13, 2014.

[3] H.-H. Hsiao, C. H. Chu, and D. P. Tsai, "Fundamentals and applications of metasurfaces," Small Methods, vol. 1, no. 4, p. 1600064, 2017.

[4] L. Zhang, S. Mei, K. Huang, and C.-W. Qiu, "Advances in full control of electromagnetic waves with metasurfaces," *Adv. Opt. Mat.*, vol. 4, no. 6, 818–833, 2016.

[5] G. Kostovski, P. R. Stoddart, and A. Mitchell, "The optical fiber tip: An inherently light-coupled microscopic platform for micro- and nanotechnologies," *Adv. Mat.* vol. 26, no. 23, pp. 3798–3820, 2014.

[6] N. Yu and F. Capasso, "Optical metasurfaces and prospect of their applications including fiber optics," *J. Lightwave Technol.*, vol. 33, no. 12, 2015.

[7] J. P. B. Mueller, "Polarization in nanophotonics," Ph.D. dissertation, Harvard Univ., Cambridge, MA, 2016.

[8] M. Principe, M. Consales, A. Micco, A. Crescitelli, G. Castaldi, E. Esposito, V. L. Ferrara, A. Cutolo, V. Galdi, and A. Cusano, "Optical fiber meta-tips," *Light Sci. Appl.*, vol. 6, no. 3, 2017.

[9] G. Calafiore, A. Koshelev, F. I. Allen, S. Dhuey, S. Sassolini, E. Wong, P. Lum, K. Munechika, and S. Cabrini, "Nanoimprint of a 3D structure on an optical fiber for light wavefront manipulation," *Nanotechnology*, vol. 27, no. 37, p. 375301, 2016.

[10] H. E. Williams, D. J. Freppon, S. M. Kuebler, R. C. Rumpf, and M. A. Melino, "Fabrication of three-dimensional micro-photonic structures on the tip of optical fibers using SU-8," *Opt. Express*, vol. 19, no. 23, pp. 22910–22922, 2011.

[11] S. Scheerlinck, P. Dubruel, P. Bienstman, E. Schacht, D. V. Thourhout, and R. Baets, "Metal grating patterning on fiber facets by UV-based nano imprint and transfer lithography using optical alignment," *J. Lightwave Technol.*, vol. 27, no. 10, pp. 1415–1420, 2009.

[12] B. Wang, T. Siahaan, M. A. Dündar, R. Nötzel, M. J. van der Hoek, S. He, and R. W. van der Heijden, "Photonic crystal cavity on optical fiber facet for refractive index sensing," *Opt. Lett.*, vol. 37, no. 5, pp. 833–835, 2012.

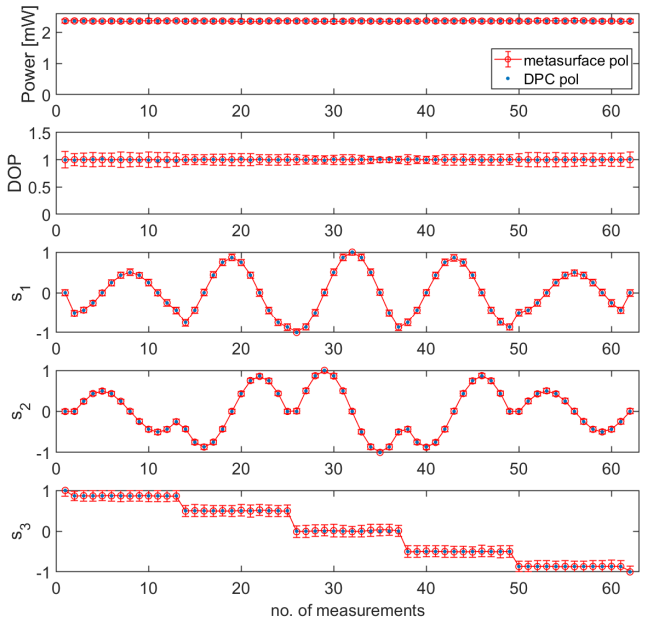

Fig. A3. Polarization measurements at 1550 nm using the fiber-based fiber exposure metasurface polarimeter.

[13] E. J. Smythe, M. D. Dickey, G. M. Whitesides, and F. Capasso, "A technique to transfer metallic nanoscale patterns to small and non-planar surfaces," *ACS nano*, vol. 3, no. 1, pp. 59–65, 2008.

[14] M. Khorasaninejad and F. Capasso, "Metalenses: Versatile multifunctional photonic components," *Science*, vol. 358, 2017.

[15] W. T. Chen, A. Y. Zhu, V. Sanjeev, M. Khorasaninejad, Z. Shi, E. Lee, and F. Capasso, "A broadband achromatic metalens for focusing and imaging in the visible," *Nat. Nanotech.*, vol. 13, pp. 220–226, 2018.

[16] A. Arbabi, E. Arbabi, S. M. Kamali, Y. Horie, S. Han, and A. Faraon, "Miniature optical planar camera based on a wide-angle metasurface doublet corrected for monochromatic aberrations," *Nat Commun.*, vol. 7, p. 13682, 2016.

[17] A. Y. Zhu, W.-T. Chen, M. Khorasaninejad, J. Oh, A. Zaidi, I. Mishra, R. C. Devlin, and F. Capasso, "Ultra-compact visible chiral spectrometer with metalenses," *APL Photonics*, vol. 2, no. 3, p. 036103, 2017.

[18] J. P. B. Mueller, K. Leosson, and F. Capasso, "Ultracompact metasurface in-line polarimeter," *Optica*, vol. 3, no. 1, pp. 42–47, 2016.

[19] N. Rubin, A. Zaidi, M. Juhl, R. Li, J. P. B. Mueller, R. Devlin, K. Leosson, and F. Capasso, "Polarization state generation and measurement with a single metasurface," *Opt. Express*, vol. 26, pp. 21455-21478, 2018.

[20] A. Pors and S. I. Bozhevolnyi, "Waveguide metacouplers for in-plane polarimetry," *Phys. Rev. Applied*, vol. 5, no. 6, p. 064015, 2016.

[21] P. S. Westbrook, T. A. Strasser, and T. Erdogan, "In-line polarimeter using blazed fiber gratings," *IEEE Photonics Technol. Lett.*, vol. 12, no. 10, pp. 1352–1354, 2000.

[22] P. Nagpal, N. C. Lindquist, S.-H. Oh, and D. J. Norris, "Ultrasmooth patterned metals for plasmonics and metamaterials," *Science*, vol. 325, no. 5940, pp. 594–597, 2009.

[23] N. Vogel, J. Zieleniecki, and I. Köper, "As flat as it gets: Ultrasmooth surfaces from template-stripping procedures," *Nanoscale*, vol. 4, no. 13, pp. 3820–3832, 2012.

[24] J. Lin, J. P. B. Mueller, Q. Wang, G. Yuan, N. Antoniou, X.-C. Yuan, and F. Capasso, "Polarization-Controlled Tunable Directional Coupling of Surface Plasmon Polaritons," *Science*, vol. 340, pp. 331–334, 2013.

[25] M. Juhl, C. Mendoza, J. P. B. Mueller, F. Capasso, K. Leosson, "Performance characteristics of 4-port in-plane and out-of-plane in-line metasurface polarimeters," *Opt. Express*, vol. 25, pp. 8697–8709, 2017.

[26] R. M. A. Azzam, "Stokes-vector and Mueller-matrix polarimetry," *J. Opt. Soc. Am. A*, vol. 33, pp. 1396–1408, 2016.

[27] B. Boulbry, J. C. Ramella-Roman, and T. A. Germer, "Improved method for calibrating a Stokes polarimeter," *Appl. Opt.*, vol. 46, pp. 8533–8541, 2007.

1077-260X (c) 2018 IEEE. Personal use is permitted, but republication/redistribution requires IEEE permission. See http://www.ieee.org/publications_standards/publications/rights/index.html for more information.

This article has been accepted for publication in a future issue of this journal, but has not been fully edited. Content may change prior to final publication. Citation information: DOI 10.1109/JSTQE.2019.2893757, IEEE Journal of Selected Topics in Quantum Electronics

[28] M. Juhl, "Metasurface Polarimetry," Ph.D. dissertation, University of Iceland, 2018.
[29] E. B. Magnusson, J. P. B. Mueller, M. Juhl, C. Mendoza, and K. Leosson, "Neural polarimeter and wavemeter," *ACS Photonics*, vol. 5, no. 7, pp. 2682–2687, 2018.
[30] A. A. Ramos and M. Collados, "Error propagation in polarimetric demodulation," Applied Optics, vol. 47, no. 14, pp. 2541–2549, 2008.
[31] J. Taylor, *An introduction to error analysis, the study of uncertainties in physical measurements.* University Science Books, 1997, pp. 209-212.

Michael Juhl received the M.Sc. degree in engineering at the Technical University of Denmark, Lyngby, Denmark, in 2003.

He has worked as a project manager and process development engineer at Alight Technologies A/S, Farum, Denmark, and is now a Ph.D student at the University of Iceland and Innovation Center Iceland, Reykjavik, Iceland, focusing on nanotechnology and metasurface polarimetry.

J. P. Balthasar Mueller received the B.Sc. degree in physics from the University of Iceland, Reykjavik, Iceland, in 2010 and the Ph.D. degree in physics from Harvard University, Cambridge, MA, in 2016.

He is associated with Harvard School of Engineering and Applied Sciences, Cambridge, MA, and is now a data scientist at Fast Forward Labs, New York City. His research focuses on nanophotonics and machine learning.

Kristjan Leosson received the B.Sc. degree in engineering physics from Queen's University, Kingston, ON, Canada, in 1994, the M.Sc. degree in technical physics from the University of Iceland, Reykjavik, Iceland, in 1996 and the Ph.D. degree in electrical engineering from the Technical University of Denmark, Lyngby, Denmark, in 2001.

He has worked as a project manager and process development engineer at Micro Manage Photons A/S, Farum, Denmark, and Lumiscence A/S, Denmark, and as a senior research scientist at the University of Iceland, focusing on fabrication of micro- and nanoscopic structures and devices. He is now the managing director of the Department of Materials, Biotechnology and Energy at the Innovation Center Iceland, Reykjavik, Iceland. He is the author of more than 70 peer-reviewed articles and is co-inventor of 4 issued patents.

1077-260X (c) 2018 IEEE. Personal use is permitted, but republication/redistribution requires IEEE permission. See http://www.ieee.org/publications_standards/publications/rights/index.html for more information.